Nanoscale Research Letters
a SpringerOpen Journal

NANO EXPRESS Open Access

Effects of photo-assisted electrodeposited on $CuInSe_2$ thin films

Tsung-Wei Chang[1*], Wen-Hsi Lee[1], Yin-Hsien Su[1] and Yu-Jen Hsiao[2]

Abstract

Photo-assisted one-step electrodeposition has been applied to help in forming smooth and dense $CuInSe_2$ films. The difference in surface morphology and crystalline quality between $CuInSe_2$ films with various photo-assistance has been investigated. In the photo-assisted electrodeposition process, the many kinds of lamps providing maximum light intensity at about 380 to 620 nm were used as light source to be irradiated onto the surface of Mo-coated soda-lime glass substrates. The results suggested effects of photo-assistance including activating surface diffusion and growing high-crystalline quality films with reduced defects during electrodeposition.

Keyword: CIS; Solar cells; Electrodeposition; Photo-assisted

Background

Chalcopyrite (CH) semiconductors have been applied as absorber layers for polycrystalline thin-film solar cells and extensively studied due to their importance in optoelectronic applications. $CuInSe_2$ (CIS) thin films are characterized as by a suitable band gap, a high absorption coefficient that exceeds 10^5 cm^{-1}, and good stability [1]. Among ternary compounds, CIS-based thin films are the most promising for use as optical absorbers for high-efficiency solar cells as they match the solar spectrum. Various methods have been used for the growth of CIS films, such as metalorganic vapor-phase epitaxy [2], molecular beam epitaxy [3], flash evaporation [4], coevaporation [5,6], and electrodeposition [7]. Several methods based on vacuum techniques have been developed to prepare CIS layers. A photo-assisted molecular beam epitaxy (MBE) process using an Hg lamp has been investigated by Tseng et al. [8]. They found that the photo-assisted MBE process dramatically reduced the epitaxial temperature to 300°C, where photons may supply an additional energy to the film surface and activate the surface diffusion and the dissociation of Se_2 and Se_4 molecules [9]. Nakada et al. [10] also proposed a laser-assisted deposition (LAD) process using the MBE system. In the process, a pulsed excimer laser (λ =248 nm) and pulsed YAG laser (λ =1,064, 532, 355, and 266 nm) were irradiated onto the substrate surface during Cu (In, Ga)Se_2 (CIGS) deposition by the three-stage process. They found the cell performance improved for all CIGS solar cells with different Ga contents, and the grain size of CIGS thin films became large and a (1 1 2)-preferred orientation was enhanced by the LAD process. The photo-assisted electrodeposition has been used to help in forming smooth and dense CIS films [10]. Accordingly, seeking possibilities for better electrodeposited film qualities, we hereby applied the photo-assistance to electrodeposition and aimed to find out the differences between electrodeposited CIS films with various wavelength photo-assistance. The crystallographic properties of CIS thin films were characterized by scanning electron microscopy (SEM), X-ray diffraction (XRD), atomic force microscopy (AFM), and Raman spectroscopy.

Methods

Mo-coated soda-lime glass substrates were washed prior to CIS growth in water containing surfactant and then rinsed with deionized water. The Mo film on the glass substrate (about 1-μm thick) was deposited by radio-frequency sputtering. Codepositions of Cu, In, and Se by the electrodeposition process were performed from a bath containing 2 mM $CuCl_2$, 25 mM $InCl_3$, 5 mM H_2SeO_3, and LiCl. The pH value was adjusted to 2 using H_2SO_4. Figure 1 shows a schematic diagram of the electrodeposition system. The rotation speed of the magnetic stirrer was set at 50 RPM. The electrochemical measurements and electrodeposition were conducted

* Correspondence: n2897109@gmail.com
[1]National Cheng Kung University, No.1, University Road, Tainan City 701, Taiwan
Full list of author information is available at the end of the article

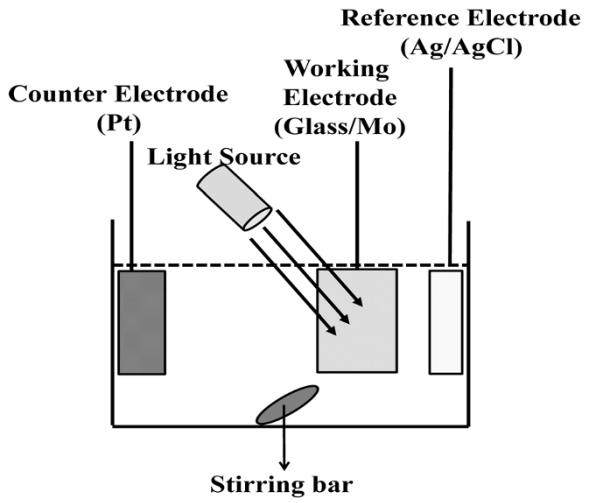

Figure 1 Schematic diagram of electrodeposition system.

using a conventional three-electrode potentiostat (AUTOLAB PGSTAT302 (Metrohm Autolab Inc., Utrecht, Netherlands)). A thin slice of a 99.99% pure Pt electrode with dimensions of 1 × 4 cm was employed as the counter electrode, and an Ag/AgCl electrode served as the reference electrode. Glass substrates with sputtered Mo film were used as the working electrode. The electrodeposition area was a square with dimensions of 1 × 1 cm. A magnetic stirrer was used for the stirring procedure. The rotation speed of the magnetic stirrer was set at 50 RPM. The potential was supplied by the potentiostat. The potential was fixed at −0.7 V. We applied the photo-assistance to electrodeposition and aimed to find out the differences between electrodeposited CIS films with various wavelength photo-assistance. The wavelengths of photo-assistance at about 380 to 476, 476 to 495, 495 to 570, 570 to 590, and 590 to 620 nm were applied to electrodeposition.

Growth experiments were performed in a room-temperature solution, under slow stirring of the bath.

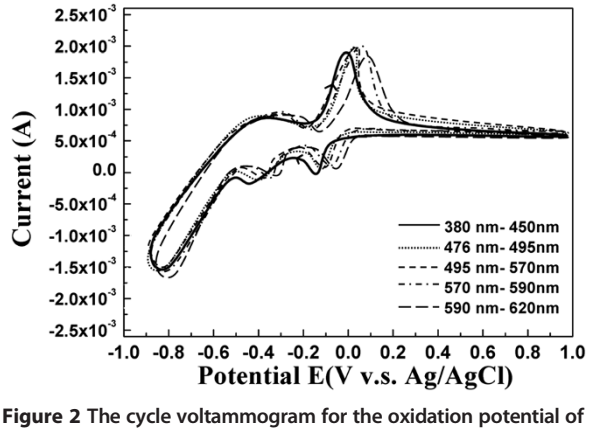

Figure 2 The cycle voltammogram for the oxidation potential of a Cu-In-Se solution for various wavelengths of photo-assistance.

Approximately 1.7-μm-thick CIS layers were obtained after 20 min of deposition. On completion of growth, CIS films were removed from the bath, rinsed with deionized water, and dried in an argon stream.

The surface morphology and chemical composition of the films were characterized by SEM (Philips XL-40FEG (Philips, Amsterdam, The Netherlands)) and energy-dispersive spectroscopy (EDS). AFM was used in contact mode. The Raman spectra were obtained in the back-scattering configuration at room temperature with unpolarized light using a spectrometer (DILOR XY 800 (J Y, Inc., Edison, NJ, USA)) and an Argon-ion laser with a 514.5-nm wavelength as the light source. The phase composition and the crystallographic structure were analyzed by XRD using a multipurpose thin-film X-ray diffractometer (Bruker D8 SSS (Bruker AXS, Inc., Madison, USA)).

Results and discussion

Figure 2 shows representative linear sweep voltammogram of Cu (II), In (III), and Se (IV) ions in a hydrochloric acid, hydrogen chloride/sodium chloride, and NaCl buffer solution with distinct photo-assistance. In the beginning, a sharp and strong cathodic peak was started at −0.1 V, which is usually attributed to the formation of Cu^+ [11]:

$$Cu^{2+} + e^- \rightarrow Cu^+ \quad (1)$$

For more negative potentials, second and third peaks were observed, which must be associated with the formation of CIS. This electrode reaction has been described as a multistep process in the literature [11,12], which results in the assimilation of In^{3+} into copper selenide, leading to the formation:

$$\begin{aligned} &Cu^+ + Se + 2e^- \rightarrow Cu_2Se \\ &2In^{3+} + 3H_2Se \rightarrow In_2Se_3 + 6H^+ \\ &Cu_2Se + In_2Se_3 \rightarrow 2CuInSe_2 \end{aligned} \quad (2)$$

Based on the above linear sweep voltammogram results, the intensities of peaks Cu_2Se and In_2Se_3 and the current density increased with various wavelengths of photo-assistance. Moreover, the reduction potential of Cu (II), $Cu_{2-x}Se$ and In_2Se_3 shifted to positive potential and prevented the evolution of H_2 when depositing CIS on the Mo substrates. On the other hand, the limit of mass transfer rate can be raised in the various wavelengths of photo-assistance, which helps replenish ions to the substrate surface. The limit of mass transfer rate is higher than the deposition rate in the various wavelengths of photo-assistance, creating a smoother surface, as shown in Figure 3a, b, c, d, e. Figure 4 shows the linear sweep voltammogram with higher Cu concentration which helps to verify the limit of mass transport effect.

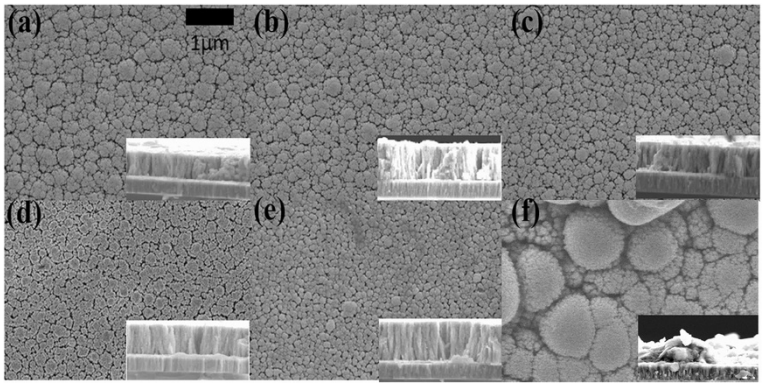

Figure 3 SEM images of CIS layer deposited at various wavelengths of photo-assistance. Wavelength at **(a)** 380 to 476 nm, **(b)** 476 to 495 nm, **(c)** 495 to 570 nm, **(d)**570 to 590 nm, **(e)** 590 to 620 nm, and **(f)** non-photo-assistance.

The increase in current density when increasing the bath concentration indicates that the deposition reaction was originally mass transfer limited. Thus an improvement in mass transfer rate is generally beneficial for the deposition process. Table 1 shows the analysis of EDS. One can observe that the Cu/In ratio rose in the various wavelengths of photo-assistance. The analysis of EDS corresponds to the linear sweep voltammogram, where the reduction potentials of Cu (II), $Cu_{2-x}Se$, and In_2Se_3 shifted positively in the various wavelengths of photo-assistance, and it obviously shifted in the wavelength of photo-assistance at about 380 to 476 nm.

The structural characterization of CIS films electrodeposited onto Mo substrates was carried out using XRD patterns within the 2θ range of 20° to 70°. XRD patterns of as-deposited CIS films in the various wavelengths of photo-assistance on Mo (1 μm)/glass substrates at −0.7 V (vs. Ag/AgCl) are presented in Figure 5. Although all peaks appear rather broad and weak which reflect a poorly crystallized material, the as-deposited films still display the three main CIS peaks; (1 1 2), (2 2 0/2 0 4), and (3 1 2/1 1 6). XRD patterns of electrodeposited CIS samples usually show peaks with broad and weak features in CIS chalcopyrite phases due to a high degree of amorphous phases and mixtures of binary and ternary compounds in the as-deposited films.

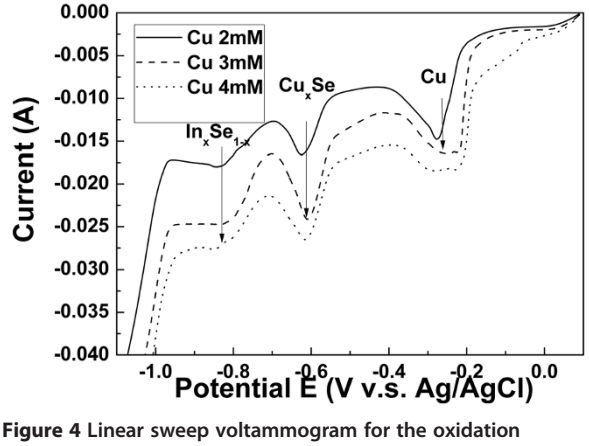

Figure 4 Linear sweep voltammogram for the oxidation potential of Cu-In-Se solution for various Cu concentrations.

The (1 1 2) peak intensity shows more crystalline CIS with increasing intensity of photo-assistance. When the intensity of photo-assistance was increased, the CIS (1 1 2) peak intensity also increased. The (1 1 2) peak intensity shows more crystalline CIS at the wavelength of photo-assistance at about 380 to 476 nm. This is presumably because of an enhanced surface migration of reduced atoms by intensity of photo-assistance. If the atoms hold a high kinetic energy on the substrate surface, they can move to appropriate positions and form a more stable lattice plane that is a closed-packed (1 1 2) plane of chalcopyrite structure [10].

Figure 6 shows the results after annealing the CIS layer at 500°C for 2 min. The following annealing step generally improves crystalline properties, resulting in well-defined sharp peaks in the XRD pattern. Clear identification of the chalcopyrite crystal structure can be achieved after the annealing step in electrodeposited CIS thin films. Figure 7 shows the full width at half maximum (FWHM) in the CIS (1 1 2) peak of the films obtained at the various wavelengths of photo-assistance. Obviously, CIS films derived

Table 1 EDS analysis of CIS layer deposited at various wavelengths of photo-assistance

Various wavelengths of photo-assistance	Cu at %	In at %	Se at %
Non-photo-assistance	17.88	19.26	62.86
380 to 476 nm	19.30	19.03	61.67
476 to 495 nm	21.58	18.49	59.94
495 to 570 nm	21.93	18.19	59.88
570 to 590 nm	18.11	19.33	62.56
590 to 620 nm	18.53	19.56	61.91

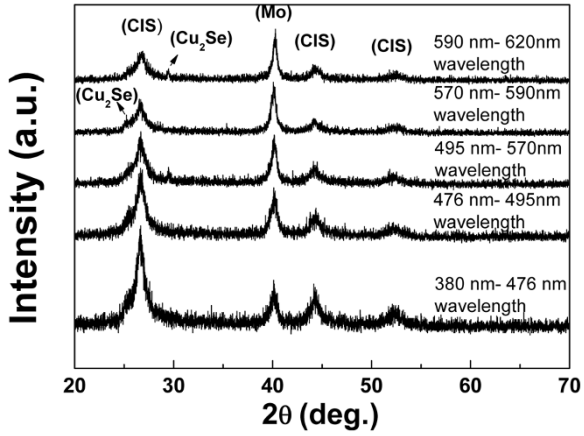

Figure 5 XRD patterns of as-deposited and annealed CIS films synthesized from Cu-In-Se solution at various wavelengths of photo-assistance.

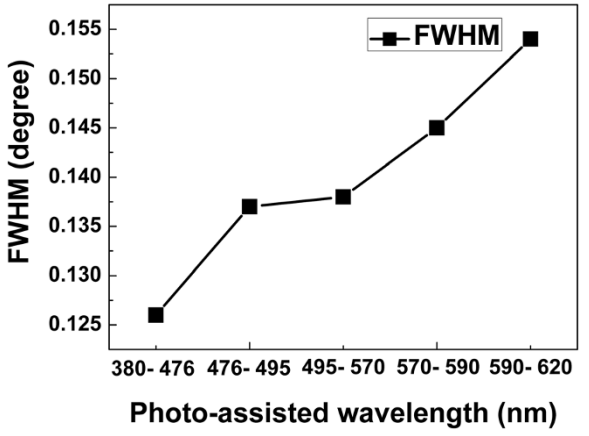

Figure 7 FWHM values of films synthesized from deposited CIS at various wavelengths of photo-assistance.

from photo-assistance with wavelength demonstrate lower FWHM values. This decrease in the FWHM is very important because it has been reported [12] that the efficiency of polycrystalline solar cells increases with decreasing FWHM for the absorbing materials. When the wavelengths of photo-assistance was reduced to 380 to 476 nm, the FWHM of the CIS (1 1 2) peak decreased to 0.126°. Moreover, because the wavelengths of photo-assistance were reduced, the electron voltage of the photo-assistance was raised to enhance surface migration of reduced atoms by photo-assistance [13].

The annealed CIS films were also analyzed by Raman spectroscopy. Figure 8 shows the Raman spectra of annealed CIS films in various wavelengths of photo-assistance in electrodeposited CIS thin films. The main part of the spectrum is situated between 100 and 300 cm^{-1}. The peak intensity of CIS CH located at A1 vibrational mode 174 cm^{-1} in the photo-assistance of near-infrared is weaker than that of CIS with the photo-assistance of near-ultraviolet. The peak intensity of CIS chalcopyrite located at E vibrational mode 216 cm^{-1} is exhibited for films in the photo-assistance of wavelengths of 380 to 476 nm and 476 to 495 nm [14]. The annealed CIS sample electrodeposited with the photo-assistance of near-infrared (570 to 590 nm and 590 to 620 nm) shows two more intense peaks; the first is situated at 240 cm^{-1} and the second at 260 cm^{-1}. The peak at 240 cm^{-1} is attributed to the presence of trigonal elementary Se [15] while the peak at 260 cm^{-1} is characteristic of Cu-Se compounds [16]. There was more crystallized CIS in photo-assistance because the electron volt of photo-assistance can enhance surface migration of reduced atoms and let CIS films be evenly deposited. In addition, this CIS surface in the photo-assistance of near-ultraviolet is smoother than the CIS surface in the

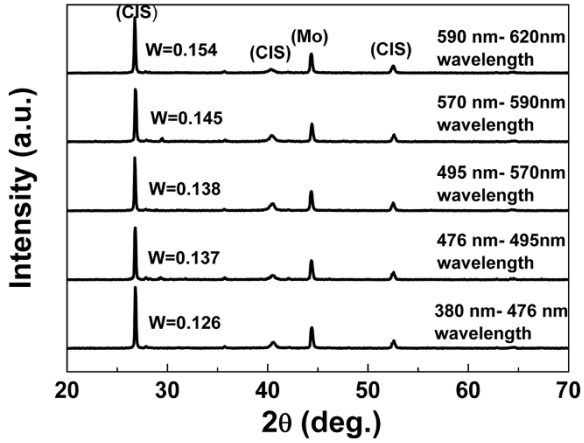

Figure 6 XRD patterns of annealed CIS films synthesized at various wavelengths of photo-assistance.

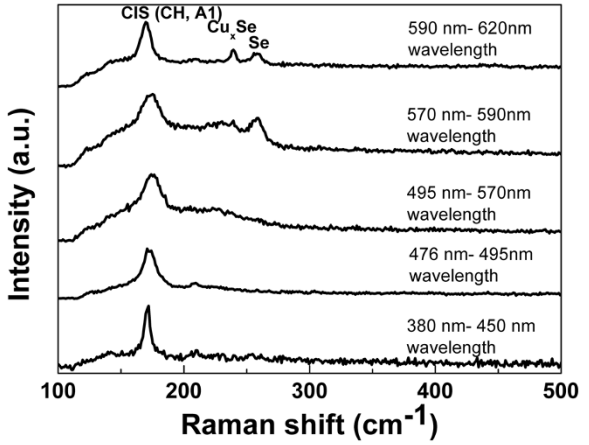

Figure 8 Raman spectra of CIS films obtained with various wavelengths of photo-assistance.

photo-assistance of near-infrared, because there is more surface migration of reduced atoms in the higher electron volt of photo-assistance.

Conclusions

In summary, we have developed a method of various wavelengths photo-assistance electrodepositing for improving morphological and crystalline qualities of CIS thin films. At the photo-assistance of wavelengths of 380 to 476 nm, smooth and dense surface morphology can be achieved due to activation of surface processes with a lower potential (−0.7 V vs. Ag/AgCl). From the XRD pattern, an enhancement in (1 1 2)-preferred orientation is observed, suggesting a formation of a closed-packed (1 1 2) plane of chalcopyrite structure. Moreover, the enhancement in crystalline quality by photo-assistance of higher electron volt remains conspicuous after the following annealing step. From Raman spectroscopy, we notice a reduction in secondary phases such as Cu-Se and Se after applying photo-assistance on CIS films deposited at −0.7 V (vs. Ag/AgCl), and the increase in intensity of peaks in Raman spectra can also be referred to a better crystalline quality. In conclusion, the higher electron volt photo-assisted electrodeposition is effective to improve not only the surface morphology but crystalline quality of electrodeposited CIS thin films.

Competing interests

The authors declare that they have no competing interests.

Authors' contributions

Study conception and design: T-WC, W-HL. Acquisition of data: T-WC. Analysis and interpretation of data: T-WC, Y-HS and Y-JH. Drafting of manuscript: T-WC. Critical revision: T-WC, W-HL. All authors read and approved the final manuscript.

Acknowledgements

This work was supported by the National Science Council of Taiwan (Grant No. NSC 103-2623-E-006-010). The authors thank National Cheng Kung University, Tainan, Taiwan, for technical support, and the University also assisted in meeting the publication costs of this article.

Author details

[1]National Cheng Kung University, No.1, University Road, Tainan City 701, Taiwan. [2]National Nano Device Laboratories, No.1, University Road, Tainan City 701, Taiwan.

Received: 23 June 2014 Accepted: 5 November 2014
Published: 9 December 2014

References

1. Luque S, Hegedus S (Eds): *Handbook of Photovoltaic Science and Engineering.* New York: Wiley; 2004.
2. Rega N, Siebentritt S, Beckers IE, Beckmann J, Albert J, Lux-Steiner M: **Defect spectra in epitaxial $CuInSe_2$ grown by MOVPE.** *Thin Solid Films* 2003, **431:**186–189.
3. Tseng BH, Lin SB, Hsieh KC, Hwang HL: **Stoichiometric control of $CuInSe_2$ thin-films using a molecular-beam epitaxy technique.** *J Cryst Growth* 1995, **150:**1206–1210.
4. Akl AAS, Ashour A, Ramadan AA, Abd El-Hady K: **Structural study of flash evaporated $CuInSe_2$ thin films.** *Vacuum* 2001, **61:**75–84.
5. Lai SC, Tseng BH, Hwang HL: **Photoluminescence in $CuGaSe_2$ thin films grown by molecular beam epitaxy.** In *Ternary and Multinary Compounds*, Institute of Physics Conference Series, Volume 152. Edited by Tomlinson RD, Hill AE, Pilkington RD. Bristol: Iop Publishing Ltd; 1998:461–464.
6. Hanna G, Mattheis J, Laptev V, Yamamoto Y, Rau U, Schock HW: **Influence of the selenium flux on the growth of Cu(In, Ga)Se_2 thin films.** *Thin Solid Films* 2003, **431:**31–36.
7. Hu SY, Lee WH, Chang SC, Cheng YL, Wang YL: **Pulsed electrodeposition of $CuInSe_2$ thin films onto Mo-glass substrates.** *J Electrochem Soc* 2011, **158:**B557–B561.
8. Tseng BH, Lin SB, Gu GL, Hsu HZ: **Interface of CuIn1-xGaxSe_2/GaAs heterostructure.** *Appl Surf Sci* 1996, **92:**412–416.
9. Ohishi M, Saito H, Okano H, Ohmori K: **Photo-assisted MBE growth of ZNSE crystals.** *J Cryst Growth* 1989, **95:**538–542.
10. Nakada T, Shirakata S: **Impacts of pulsed-laser assisted deposition on CIGS thin films and solar cells.** *Sol Energy Mater Sol Cells* 2011, **95:**1463–1470.
11. Oliveira MCF, Azevedo M, Cunha A: **A voltammetric study of the electrodeposition of $CuInSe_2$ in a citrate electrolyte.** *Thin Solid Films* 2002, **405:**129–134.
12. Minemoto T, Wakisaka Y, Takakura H: **Grain boundary character distribution on the surface of Cu(In, Ga)Se_2 thin film.** *Jpn J Appl Phys* 2011, **50:**4.
13. Dejene FB: **Material and device properties of Cu(In, Ga)Se_2 absorber films prepared by thermal reaction of InSe/Cu/GaSe alloys to elemental Se vapor.** *Curr Appl Phys* 2010, **10:**36–40.
14. Tanino H, Maeda T, Fujikake H, Nakanishi H, Endo S, Irie T: **Raman-spectra of $CuInSe_2$.** *Phys Rev B* 1992, **45:**13323–13330.
15. Ramdani O, Guillemoles JF, Lincot D, Grand PP, Chassaing E, Kerrec O, Rzepka E: **One-step electrodeposited $CuInSe_2$ thin films studied by Raman spectroscopy.** *Thin Solid Films* 2007, **515:**5909–5912.
16. Ishii M, Shibata K, Nozaki H: **Anion distributions and phase-transitions in cus1-xsex(x =0-1) studied by Raman spectroscopy.** *J Solid State Chem* 1993, **105:**504–511.

doi:10.1186/1556-276X-9-660
Cite this article as: Chang *et al.*: Effects of photo-assisted electrodeposited on $CuInSe_2$ thin films. *Nanoscale Research Letters* 2014 **9**:660.